Forward Skirt Structural Testing on the Space Launch System (SLS) Program

J.D. Lohrer, R.D. Wright
Orbital ATK Propulsion Systems, Promontory, Utah

Structural testing was performed to evaluate heritage forward skirts from the Space Shuttle program for use on the Space Launch System (SLS) program. One forward skirt is located in each solid rocket booster as shown in Figure 1. Heritage forward skirts are aluminum 2219 welded structures as shown in Figure 2. Loads are applied at the forward skirt thrust post and ball assembly as shown in Figure 3. Testing was needed because SLS ascent loads are roughly 40% higher than Space Shuttle loads. Testing objectives were to determine margins of safety, demonstrate reliability, and validate analytical models.

Two forward skirts were structurally tested using the test configuration shown in Figure 4. The test stand applied loads to the thrust post as shown in Figure 5. Four hydraulic actuators were used to apply axial load and two hydraulic actuators were used to apply radial and tangential loads.

The first test was referred to as FSTA-1 (Forward Skirt Structural Test Article) and was performed in April/May 2014. The purpose of FSTA-1 was to verify the ultimate capability of the forward skirt subjected to ascent ultimate loads. Testing consisted of two liftoff load cases taken to 100% limit load followed by an ascent load case taken to 110% limit load. The forward skirt was unloaded to no load after each test case. Lastly, the forward skirt was tested to 140% limit and then to failure using the ascent loads.

The second test was referred to as FSTA-2 and performed in July/August of 2014. The purpose of FSTA-2 was to verify the ultimate capability of the forward skirt subjected to liftoff ultimate loads. Testing consisted of six liftoff load cases taken to 100% limit load followed by the six liftoff cases taken to 140% limit load. Two ascent load cases were then tested to 100% limit load. The forward skirt was unloaded to no load after each test case. Lastly, the forward skirt was tested to 140% limit and then to failure using the ascent loads.

The forward skirts on FSTA-1 and FSTA-2 successfully carried all applied liftoff and ascent load cases. Both FSTA-1 and FSTA-2 were tested to failure by increasing the ascent loads. Failure occurred in the forward skirt thrust post radius as shown in Figures 6 and 7. The forward skirts on FSTA-1 and FSTA-2 had nearly identical failure modes. FSTA-1 failed at 1.72 times limit load and FSTA-2 failed at 1.62 times limit load. This difference is primarily attributed to variation in material properties in the thrust post region.

Test data were obtained from strain gages, deflection gages, ARAMIS digital strain measurement, acoustic emissions, and high-speed video. Strain gage data and ARAMIS strain were compared to finite element (FE) analysis predictions. The FE model is shown in Figures 8 and 9. Both the forward skirt and tooling were modeled. This allows the analysis to simulate the loading as close as possible to actual test configuration.

FSTA-1 and FSTA-2 were instrumented with over 200 strain gages to ensure all possible failure modes could be captured. However, it turned out that three gages provided critical strain data. One was located in the post bore and two on the post radius as shown in Figure 10. More gages were not specified due to space limitations and the desire to not interfere with the use of the ARAMIS system on the post radius. Measured strains were compared to analysis results for the load cycle to failure as shown in Figures 11 through 14. Note that FSTA-1 gages were lost before failure was reached. FSTA-2 gages made it to the failure load but one of the radius gages was lost before testing began. This gage was not replaced because of the time and cost associated with disassembly of the test structure. Correlation to analysis was excellent for FSTA-1. FSTA-2 was not quite as good because there was more residual strain from previous load cycles. FSTA-2 was loaded and unloaded with 12 liftoff cases and two ascent cases before taking the skirt to failure. FSTA-1 only had two liftoff cases and one ascent case before taking the skirt to failure.

The ARAMIS system was used to determine strain at the post radius by processing digital images of a speckled paint pattern. Digital cameras shown in Figure 15 recorded images of the speckled paint pattern shown in Figure 16. ARAMIS strain results are shown in Figure 17 for FSTA-2 just prior to failure. Note a high strain location develops near the left side. This high strain compares well to analysis prediction for both FSTA-1 and FSTA-2 as shown in Figure 18. The strain at this location was also plotted versus limit load in Figures 19 and 20. Both FSTA-1 and FSTA-2 had excellent correlation between ARAMIS and analysis strains.

Acoustic emission (AE) sensors were used to monitor for damage formation that may occur during testing (e.g., crack formation and growth or propagation). AE was very important because after disassembly of FSTA-1, a crack was observed in the ball fitting radius as shown in Figure 21. The ball fitting did not crack on FSTA-2. AE data was

used to reconstruct when the crack occurred. The AE energy versus time plot for FSTA-1 is shown in Figure 22. The energy increased considerably at 850 seconds (152% limit load), indicating a crack could have formed at this point. The only visual evidence found that could have corresponded to this was the crack that initiated in the ball fitting. The cracks in the forward skirt aluminum structures would likely have been lower energy due to a lower modulus and all that were found after failure correlated to occurring after the initial crack in the post radius. This was verified by high-speed cameras used to record the failure.

In summary, testing of the heritage forward skirt was a success. Testing proved the forward skirts were acceptable to use on the SLS program. This saved the SLS program approximately 30 million dollars because new forward skirts did not need to be designed, tested, and manufactured.

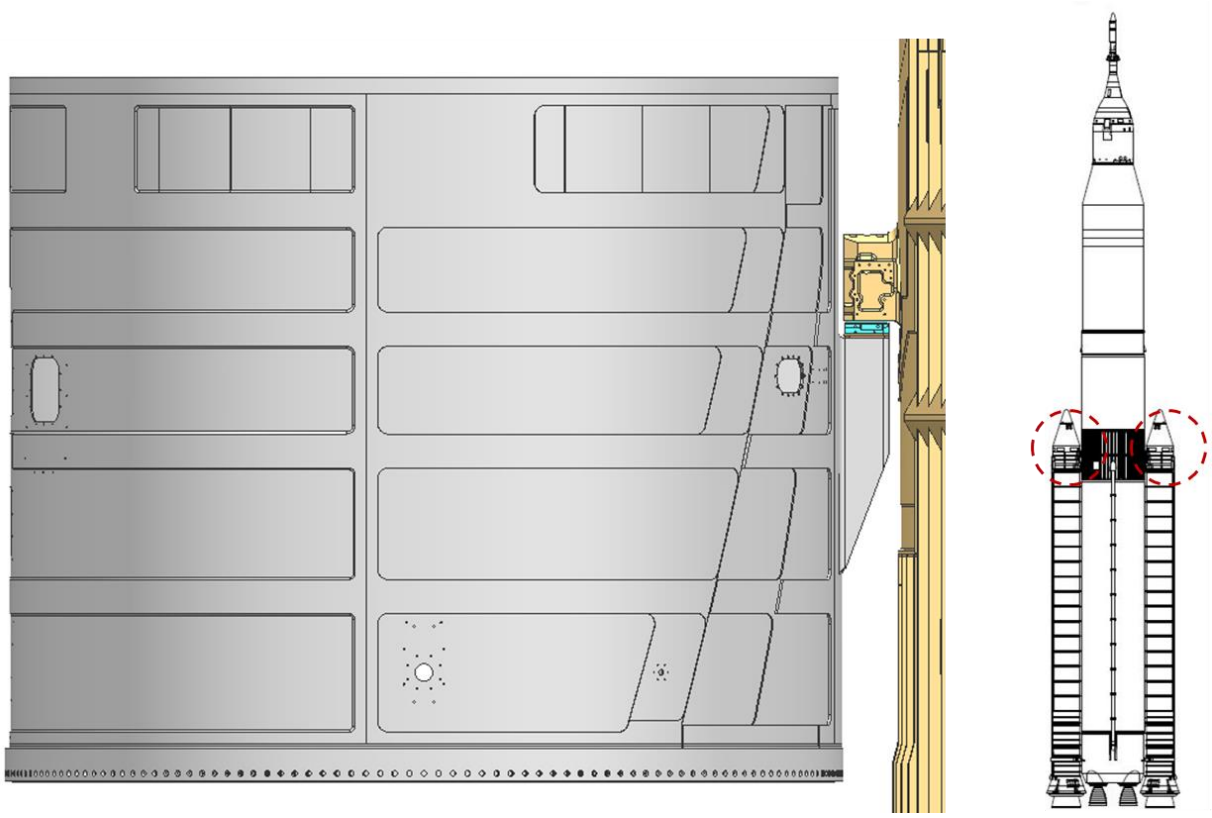

Figure 1. SLS forward skirt location.

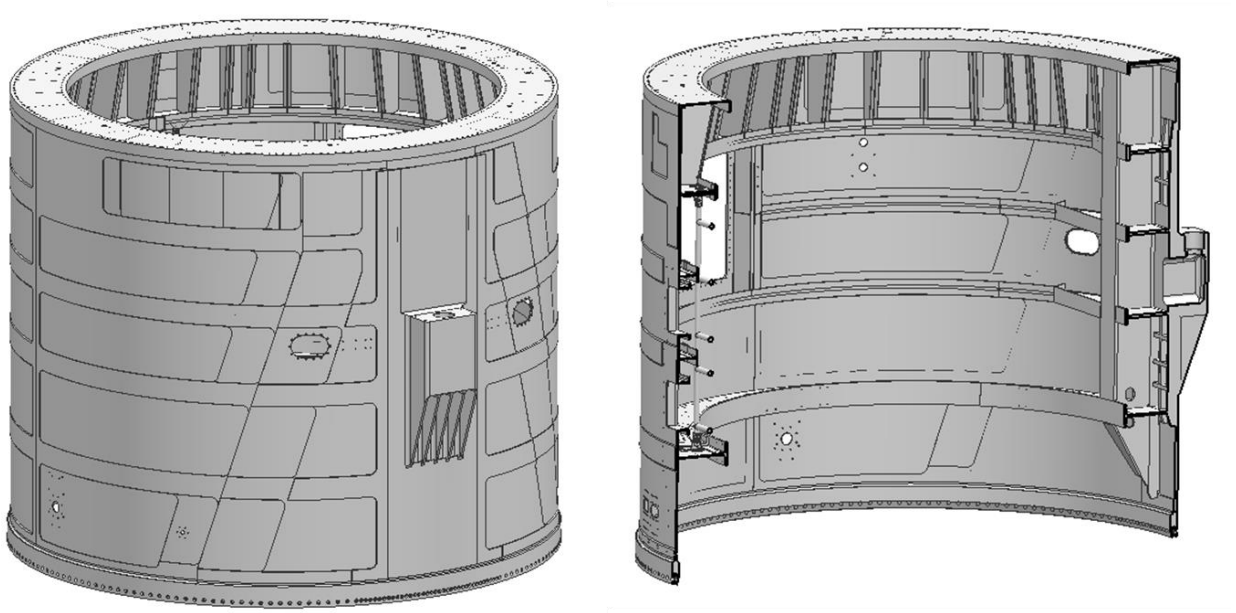

Figure 2. SLS forward skirt.

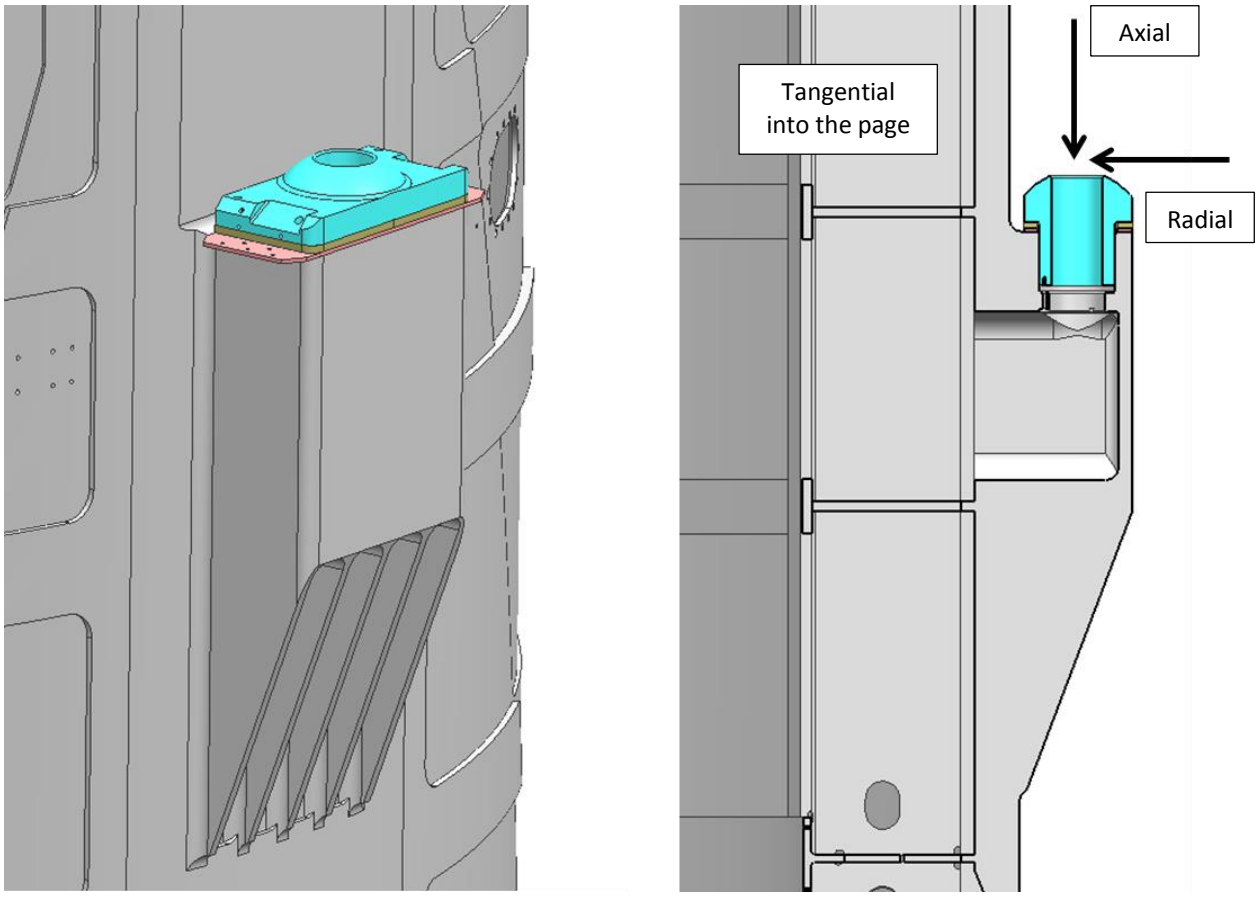

Figure 3. Forward skirt loads.

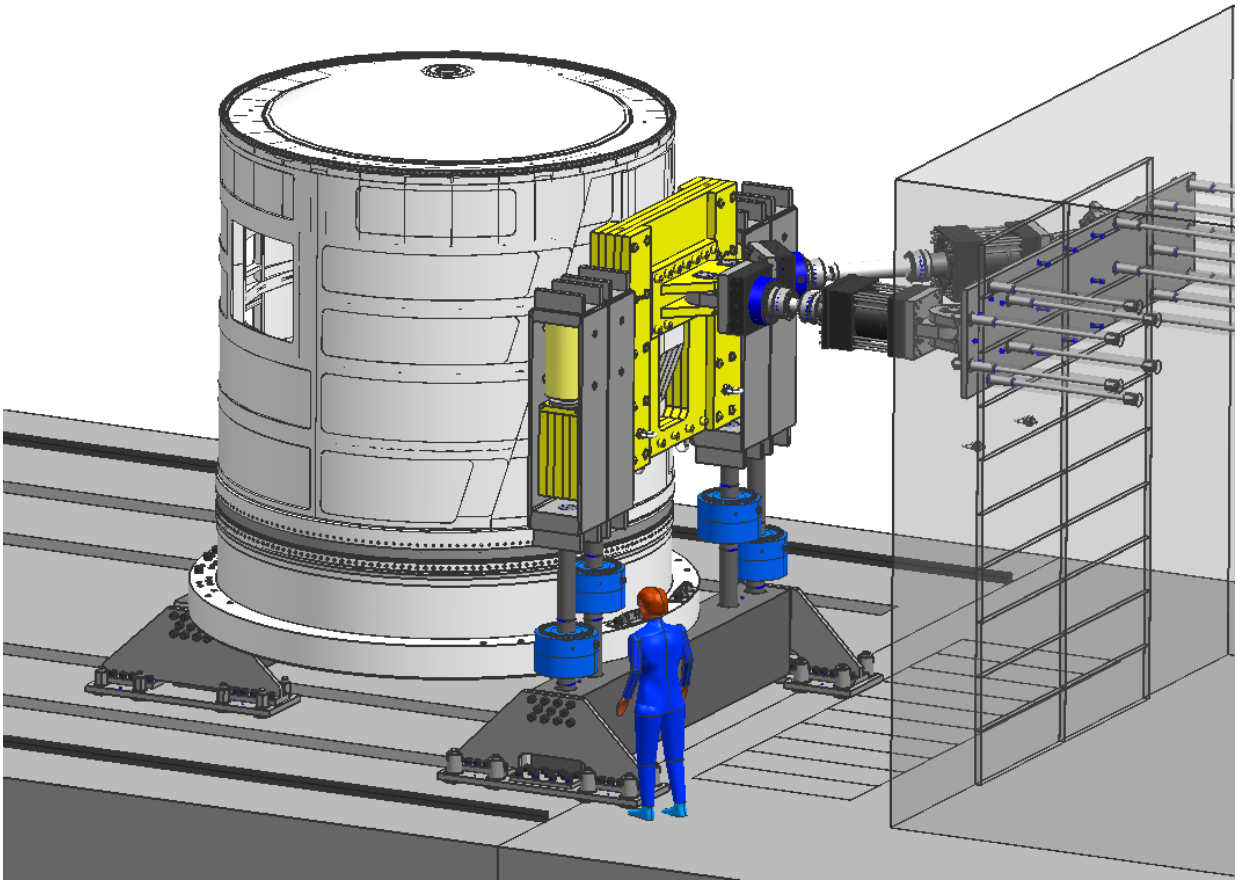

Figure 4. Test configuration.

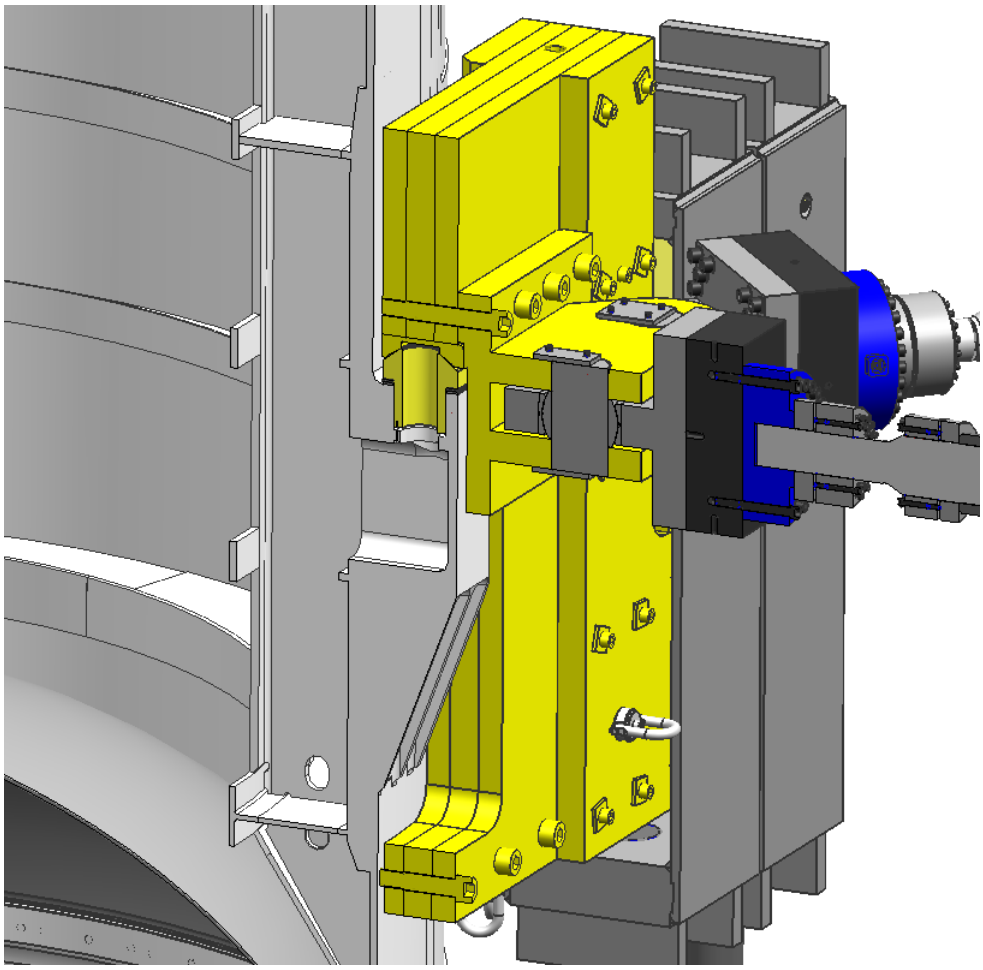

Figure 5. Cross-sectional view of load application on thrust post.

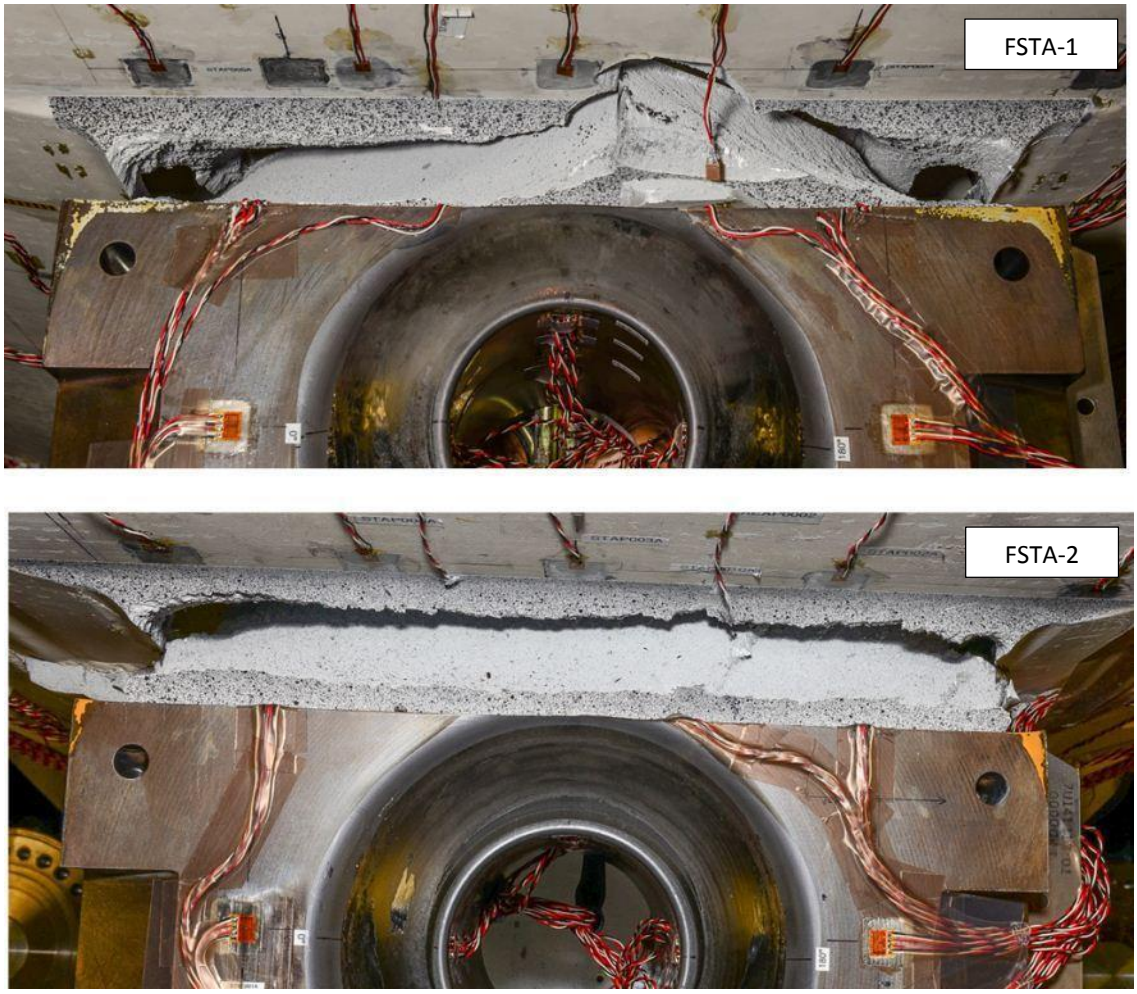

Figure 6. Top view of failure.

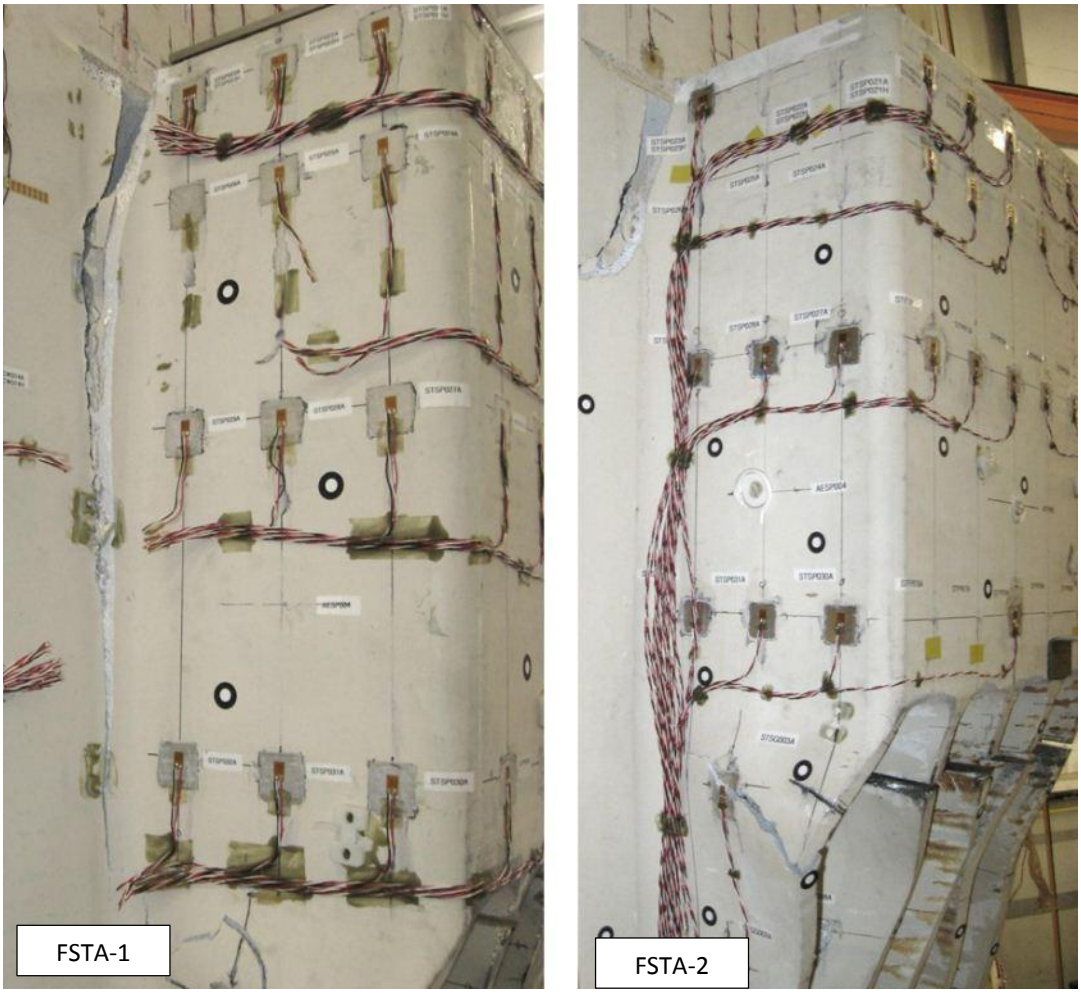

Figure 7. Right side view of post failure.

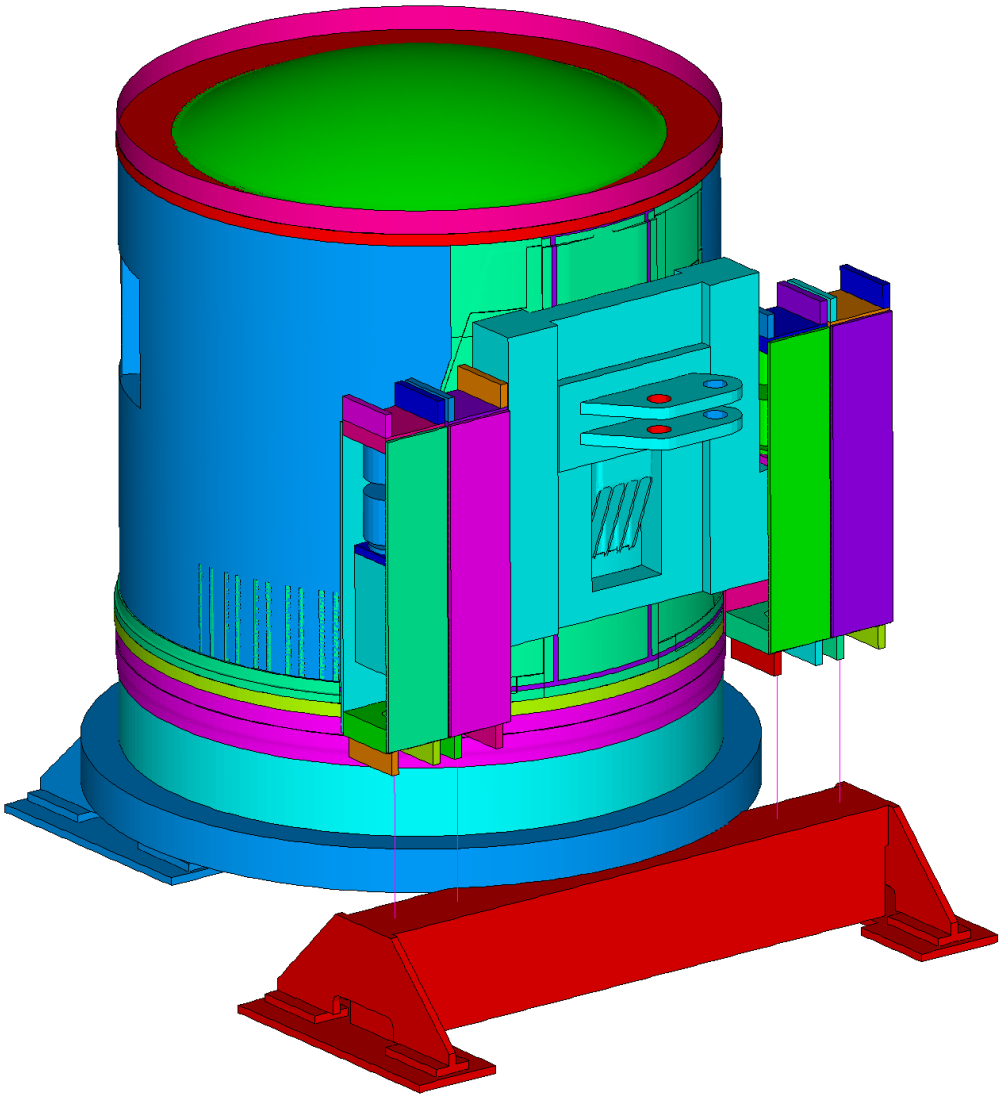

Figure 8. FSTA FE model.

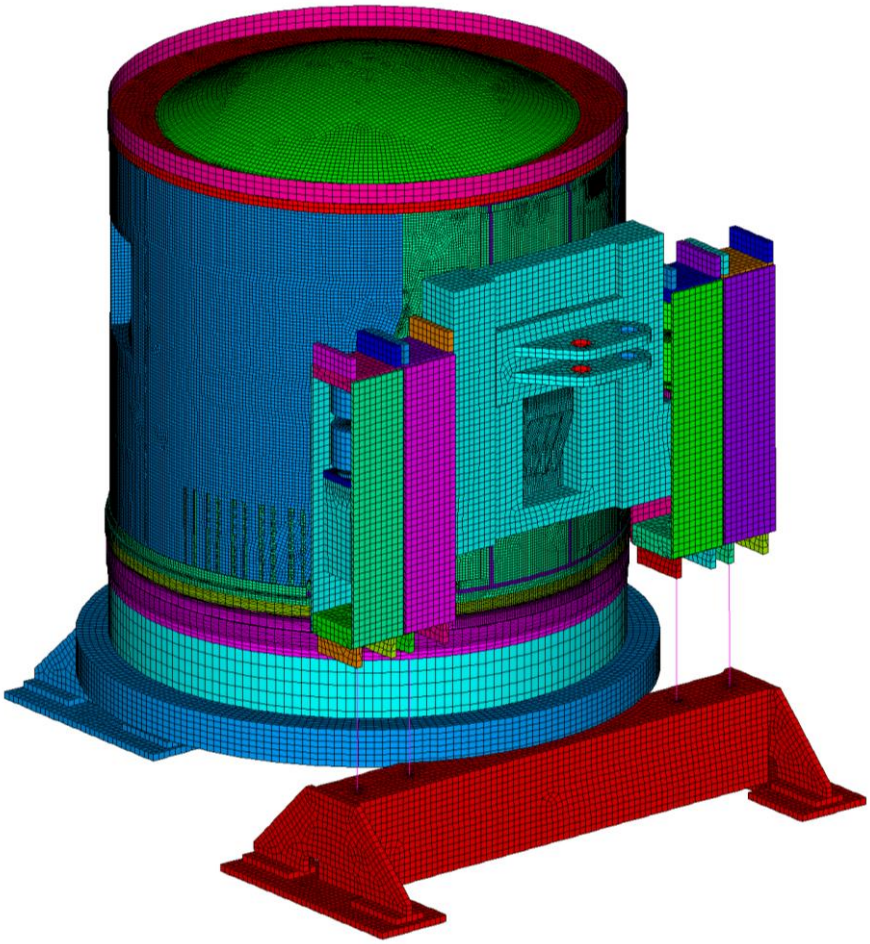

Figure 9. FSTA FE model mesh density.

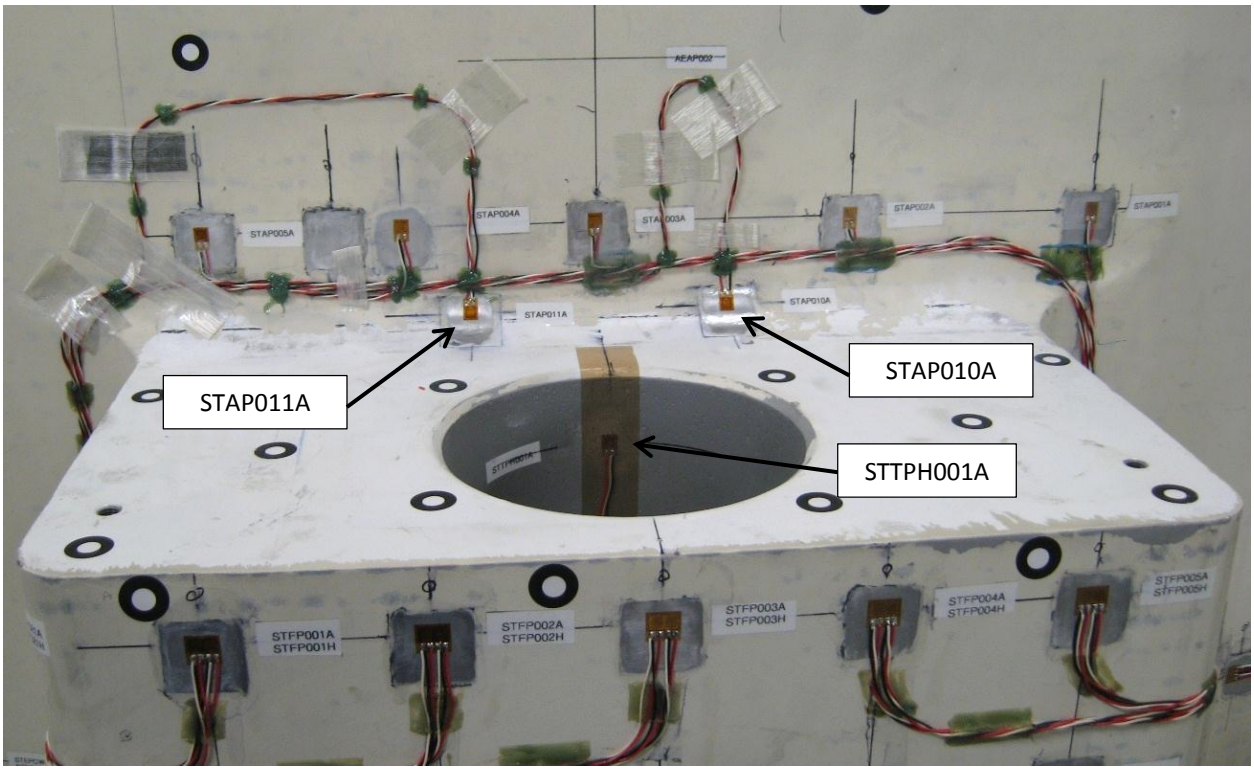

Figure 10. Critical strain gages.

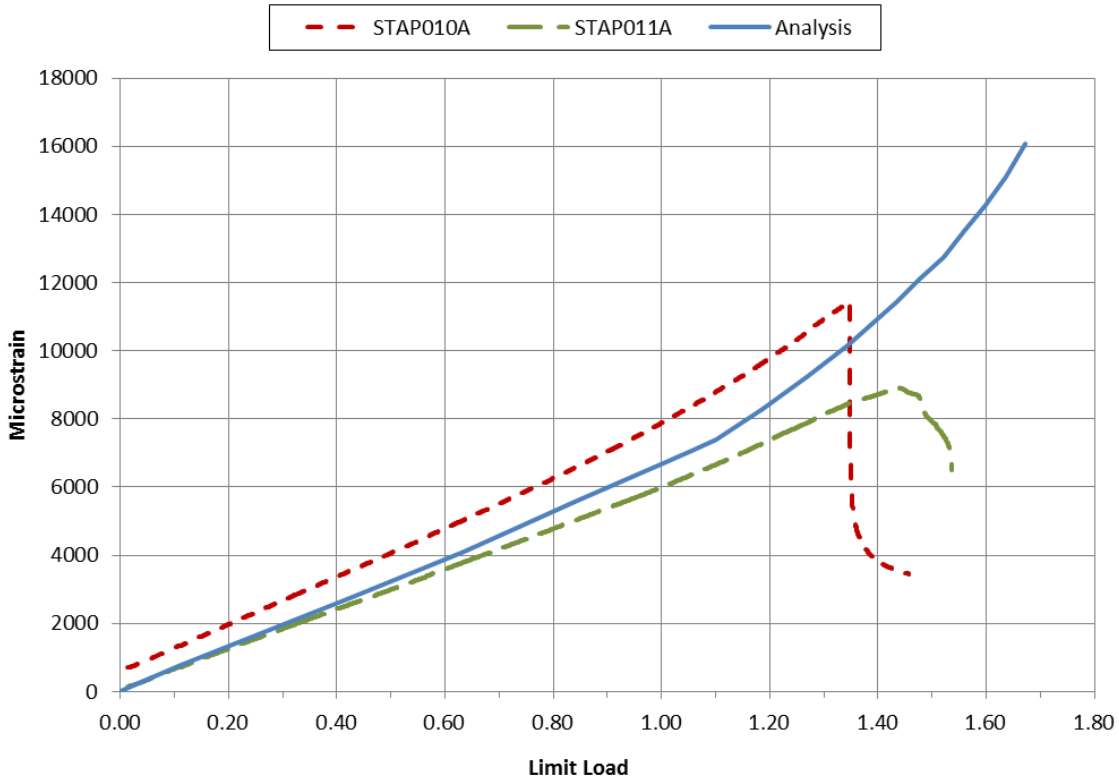

Figure 11. FSTA-1 radius gage strains.

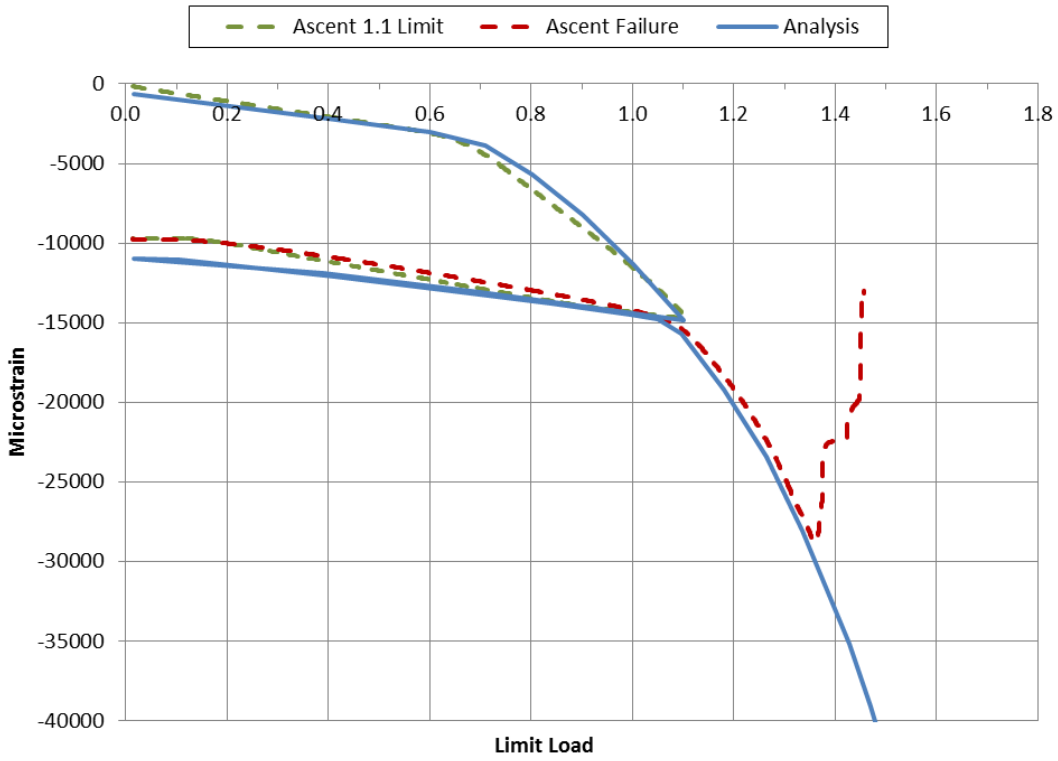

Figure 12. FSTA-1 bore gage strains.

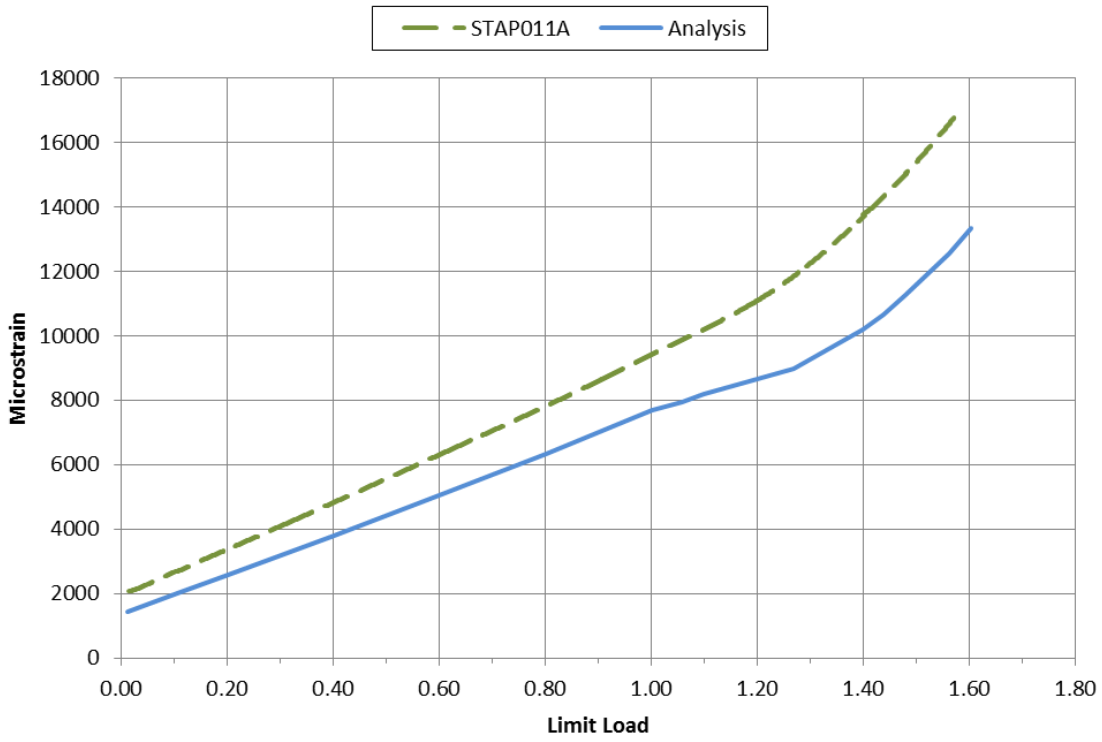

Figure 13. FSTA-2 radius gage strains.

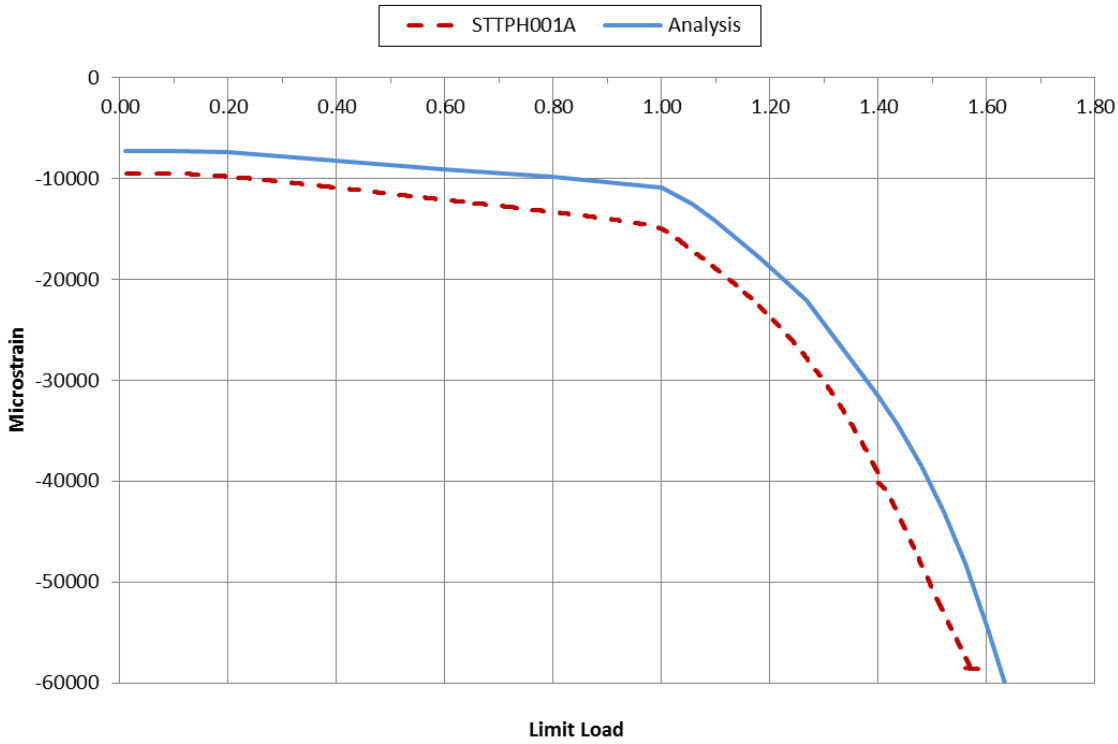

Figure 14. FSTA-2 bore gage strains.

Figure 15. ARAMIS digital cameras viewing post radius.

Figure 16. Post radius speckle pattern.

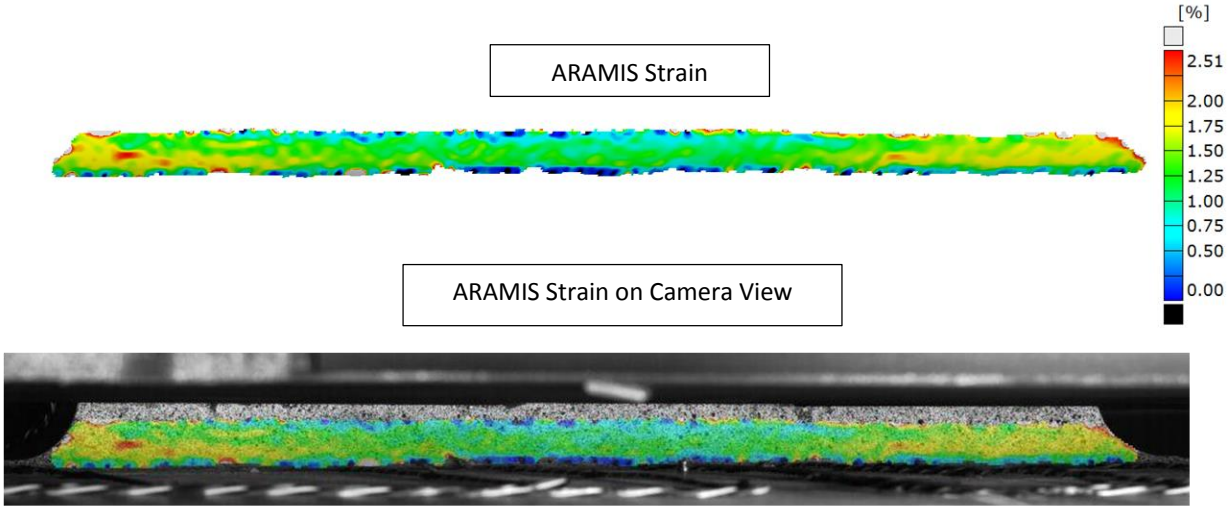

Figure 17. FSTA-2 ARAMIS strain contour.

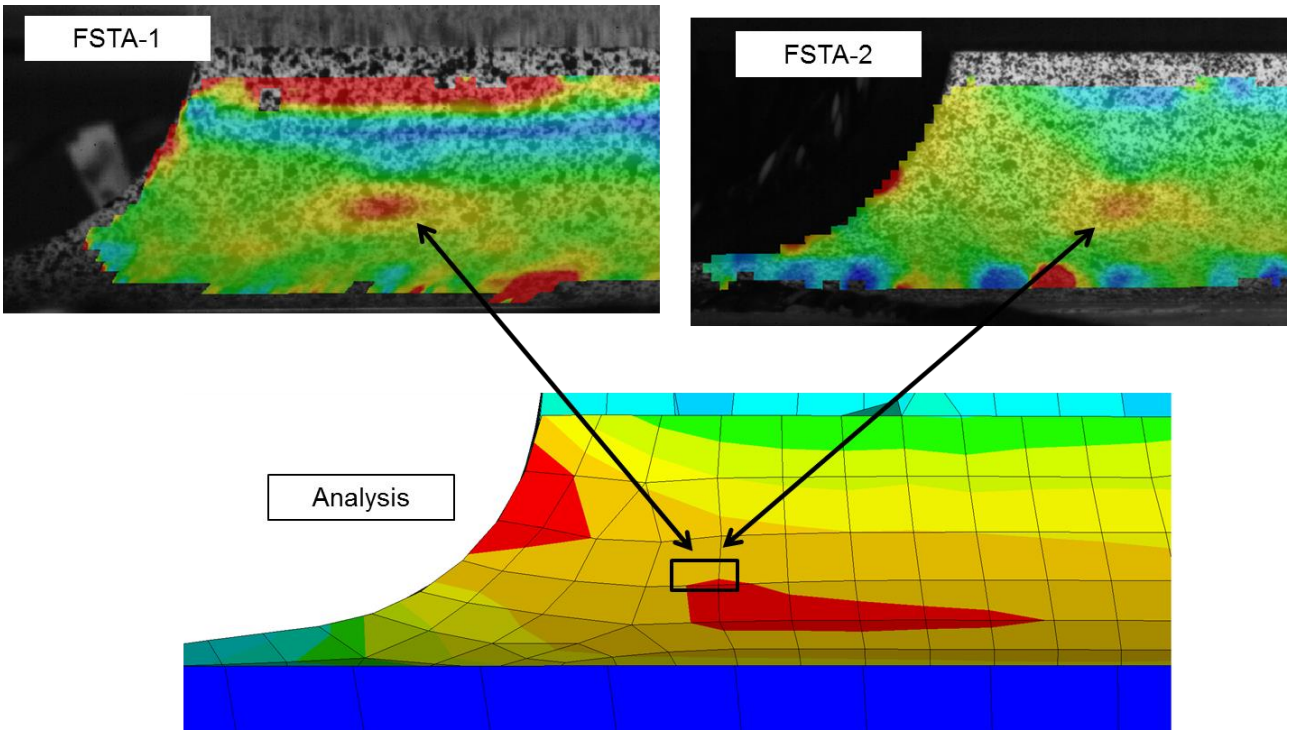

Figure 18. ARAMIS versus analysis strain at hot spot.

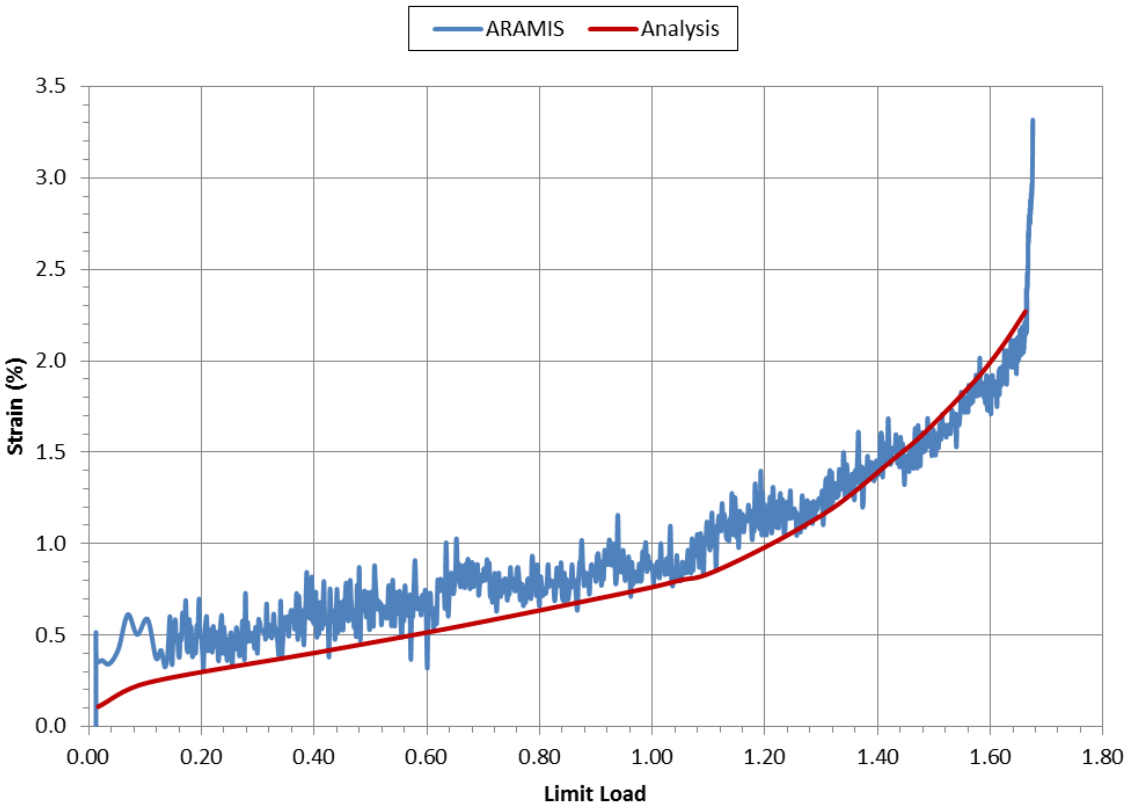

Figure 19. FSTA-1 ARAMIS versus analysis strain.

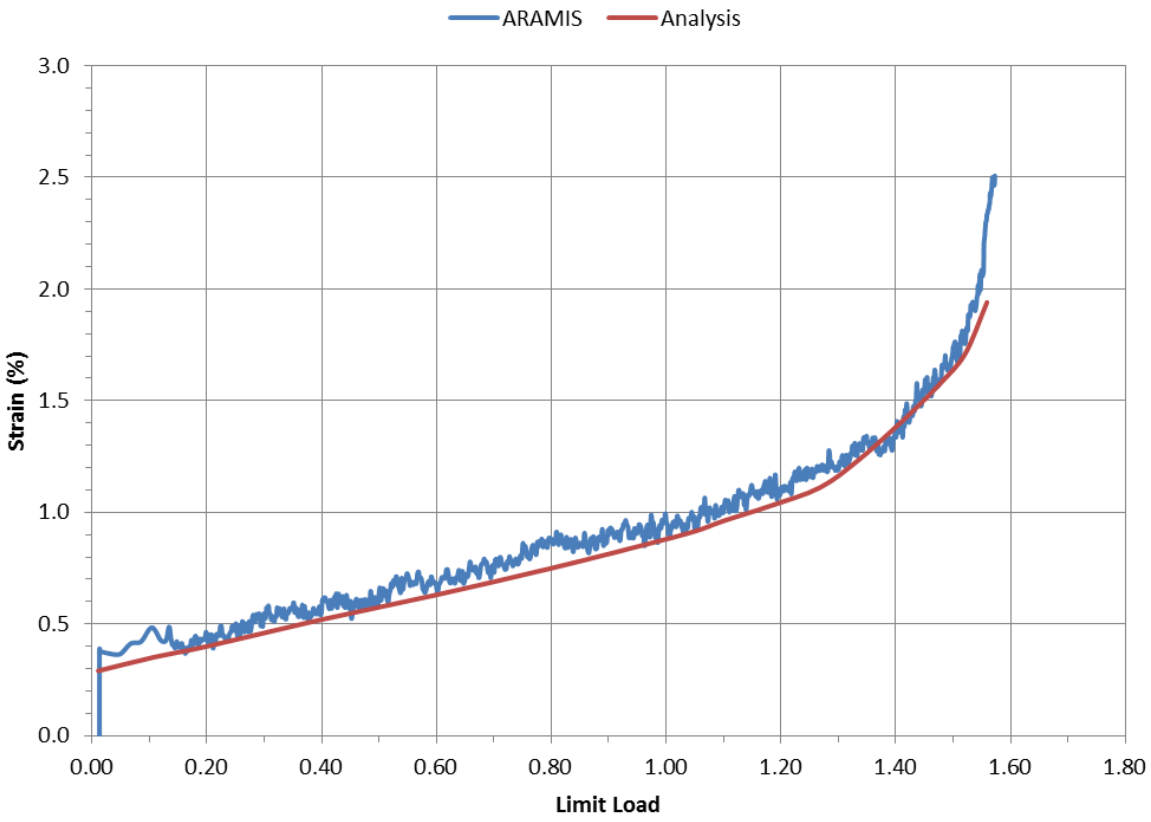

Figure 20. FSTA-2 ARAMIS versus analysis strain.

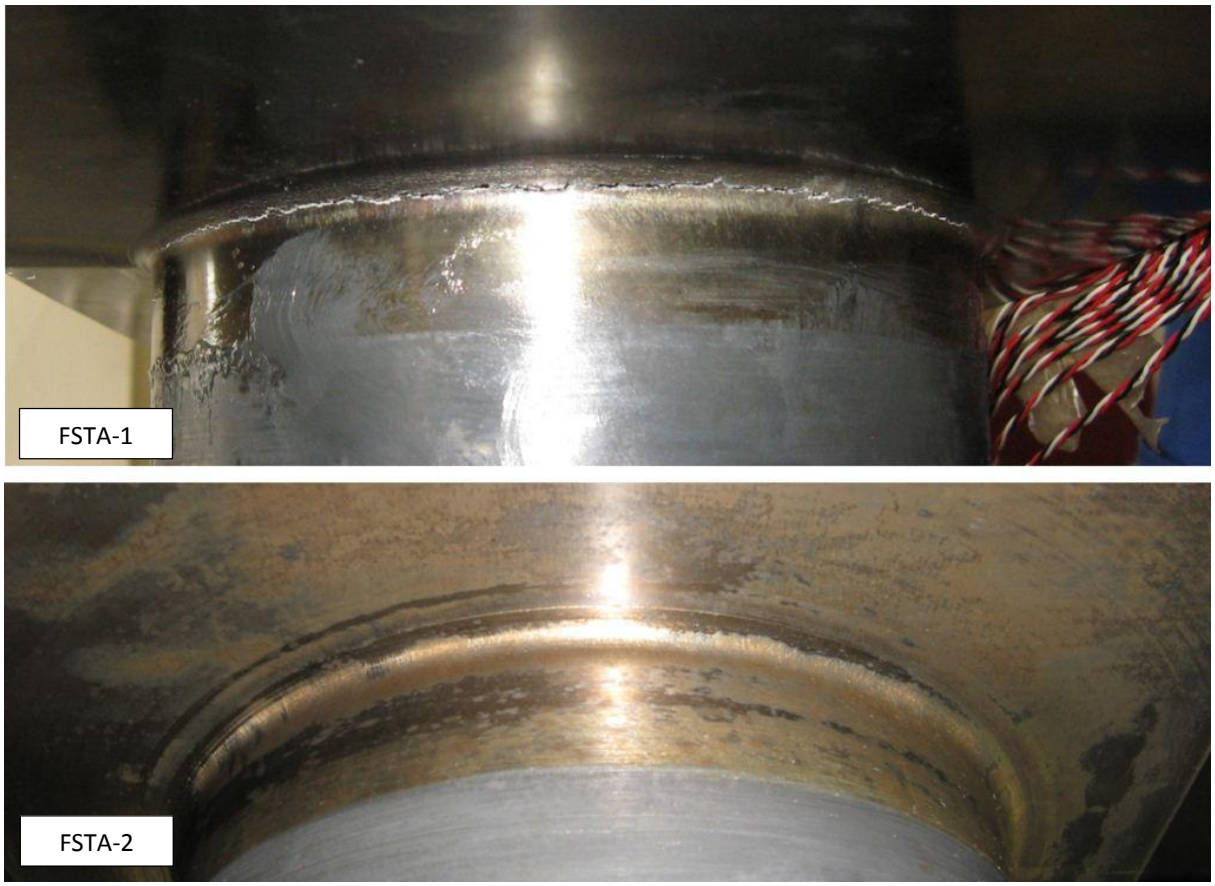

Figure 21. Ball fitting radius.

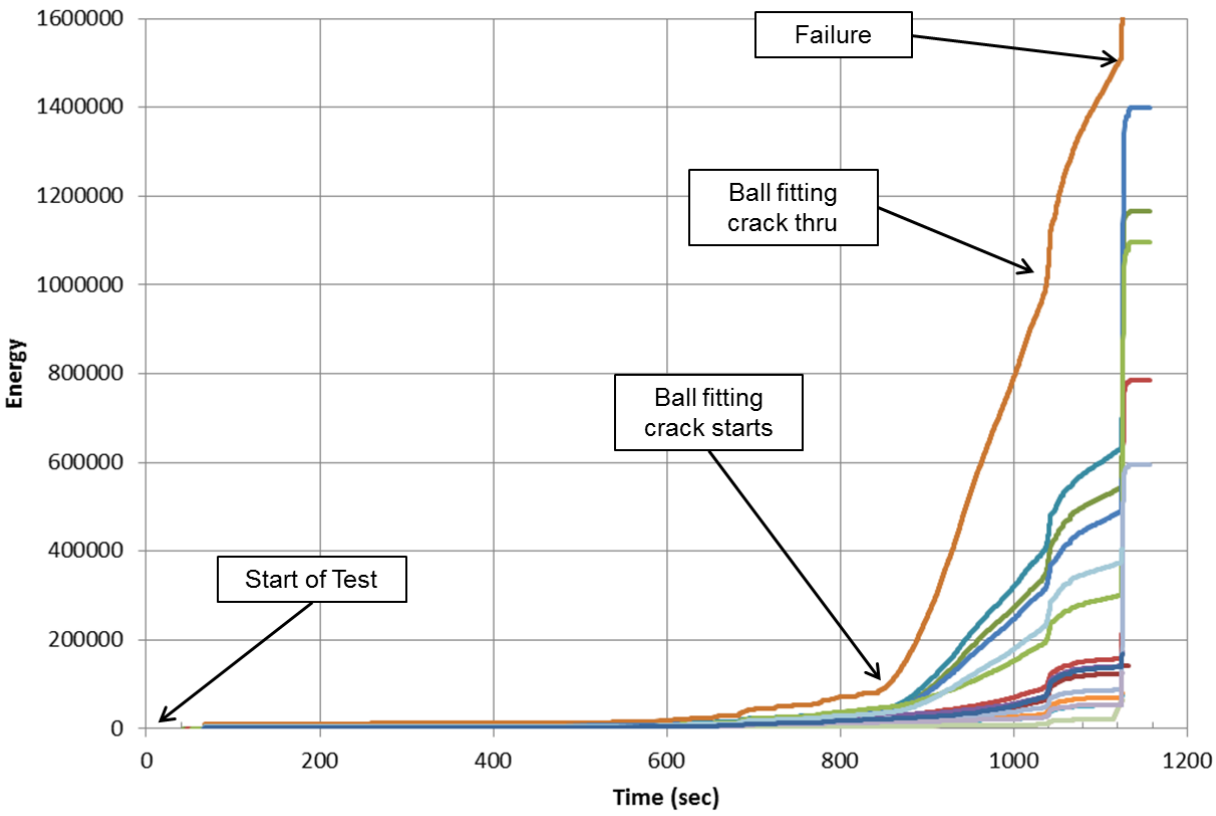

Figure 22. FSTA-1 acoustic energy events.